Invited Paper

Anticipatory control using substrate manipulation enables trajectory control of legged locomotion on heterogeneous granular media

Feifei Qian[a] and Daniel Goldman[b]

[a]School of Electrical and Computer Engineering,
[b]School of Physics,
Georgia Institute of Technology, Atlanta, USA

ABSTRACT

Legged robots must traverse complex terrain consisting of particles of varying size, shape and texture. While much is known about how robots can effectively locomote on hard ground and increasingly on homogeneous granular media, principles of locomotion over heterogeneous granular substrates are relatively unexplored. To systematically discover how substrate heterogeneity affects ambulatory locomotion, we investigate how the presence of a single boulder (3D printed convex objects of different geometries) embedded in fine granular media affects the trajectory of a small (150 g) six legged robot. Using an automated system to collect thousands of locomotion trials, we observed that trajectories were straight before the interaction with the boulder, and scattered to different angles after the interaction depending on the leg-boulder contact positions. However, this dependence of scattering angle upon contact zone was relatively insensitive to boulder shape, orientation and roughness.[1] Inspired by this insensitivity, here we develop an anticipatory control scheme which uses the scattering information in coordination with a tail induced substrate jamming. Our scheme allows the robot to "envision" outcomes of the interaction such that the robot can prevent trajectory deviation before the scattering occurs. We hypothesize that (particularly during rapid running or in the presence of noisy sensors) appropriate substrate manipulation can allow a robot to remain in a favorable locomotor configuration and avoid catastrophic interactions.

Keywords: robot locomotion, heterogeneous granular ground

1. INTRODUCTION

Legged locomotors in the biological world combine sensory information and prior knowledge to perform anticipatory obstacle negotiation on challenging heterogeneous terrains.[3] In particular, we are interested to understand how animals like the Zebra-tailed lizard (Fig. 1A) which live in heterogeneous granular terrain locomote so effectively in the presence of particulates of widely varying sizes (from micro-scale fine particles to rocks comparable to body height). While little is known about animal locomotion in such terrain, in the past $\sim$ 10 years, there have been a number of biological studies that demonstrate that animals can use a combination of preflexive and "anticipatory" control (integrating muscle function, body dynamics and neuromuscular control) to achieve graceful locomotion on terrain possessing obstacles, gaps, etc.[3–7]

Among robotic locomotors, such anticipatory control schemes could be useful in traversing heterogeneous terrain. Such terrain is common in particulate substrates like deserts or Martian terrain (Fig. 1B,C) – these landscapes are often composed of collections of particles of different sizes and shapes. When even well controlled legged robotic locomotors, like the RHex shown in Fig. 1B, travel across these heterogeneous granular environments, they exhibit failure modes like slips, unstable foot-holds, impassable barriers, etc. Such terrain mismanagement significantly affects robot stability, trafficability and power consumption.

Further author information: (Send correspondence to Daniel I. Goldman)
Daniel I. Goldman: E-mail: daniel.goldman@physics.gatech.edu

Micro- and Nanotechnology Sensors, Systems, and Applications VII, edited by Thomas George, Achyut K. Dutta, M. Saif Islam, Proc. of SPIE Vol. 9467, 94671U · © 2015 SPIE
CCC code: 0277-786X/15/$18 · doi: 10.1117/12.2177224

Figure 1. Natural heterogeneous granular terrain and locomotion challenges on such substrates. (A) The Zebra-tailed lizard (*C. draconoides*) runs rapidly over a diversity of such terrain (photo courtesy YouTube[2]). (B) RHex robot traveling across heterogeneous gravel substrate (photo courtesy Alfred Rizzi, Boston Dynamics). (C) A representative example of natural heterogeneous granular substrate, a view of the Martian terrain taken by the Curiosity Rover (photo courtesy NASA). As seen from the photo the substrate consists of multi-shape and multi-size particles, from fine sand and small gravel to large rocks.

Obstacle-interactive locomotion strategies are relatively unexplored for robotic locomotors. Currently, most terrestrial vehicles (including mobile robots) are tested on either hard ground or substrates composed of standardized homogenous media like Ottowa sand[8] and lunar simulants.[9] Many traditional navigation planning methods for navigation in obstacle environments involve finding a "collision free" path, which requires the robot to avoid obstacles. This is reasonable for most wheeled/treaded robots which must circumvent obstacles, but for legged robots, traversing obstacles by stepping over or upon them[10] can be a valid and possibly even a more effective option. Allowing robots to gracefully interact with obstacles[11] opens a new avenue for strategic navigation planning, and could significantly expand viable exploration space for obstacle-filled environments as well as aid robots in time critical tasks like search and rescue.

Development of obstacle-interactive legged robot locomotion control on heterogeneous granular terrain requires fundamental understanding of the complex interactions between the robot and the heterogeneous ground, which can be especially complicated when ground heterogeneities possess mobility relative to the substrates underneath. One of the challenges in creating the next generation of mobile robots is creating a discipline that can expand the scope of terramechanics[12,13] from large tracked and treaded vehicles on homogeneous ground to arbitrarily shaped and actuated (e.g. limbs,[14] flippers,[15] body undulators[16,17]) locomotors moving on and within complex heterogeneous terrestrial substrates; we refer to this generalizaton as "terradynamics". Both terramechanics and our recent terradynamic Resistive Force Theory models[18] can model locomotion on homogeneous substrates largely because interaction models are smooth and deterministic. However, in typical heterogeneous environments, the force fluctuations introduced by heterogeneities (gravel, rocks, boulders, etc.) during intrusion and drag can be large, which makes the applicability of continuum based approaches like terramechanics[12,13] and resistive force theory unclear.

To move toward a terradynamics of heterogeneous terrain, previously we designed and constructed the SCATTER system[19] (Systematic Creation of Arbitrary Terrain and Testing of Exploratory Robots) to automatically create heterogeneous granular ground conditions and perform robot locomotion tests within these environments. Using SCATTER, we investigated the locomotor dynamics during interaction with a single 3D printed convex objects of different geometries, textures, burial depths and mobilities.[1] Our study revealed that the complex interaction between a robot with a single boulder could be modelled as a scattering process – depending on the contact position on the boulder, the robot left the heterogeneity with a certain angle of trajectory deviation.

In this paper, we demonstrate that using the scattering information as prior knowledge, the robot can statistically estimate the outcomes of the interaction and thus perform an anticipatory correction to avoid catastrophic interaction modes and large course deviation. In particular, we rely on use of the solid-fluid transition in the granular media to effect a simple control scheme to manipulate the world: a deeply penetrated tail induces a granular media solidification, which enables a kinematically constrained body reorientation that corrects for the trajectory deviation caused by the scattering event. Our results thus indicate that the control of terrestrial locomotion can be simplified through manipulation of the environment.

2. A REVIEW OF THE SCATTER SYSTEM

Here we briefly review the experimental apparatus which was previously developed and is used in this paper. In [19] , we developed a fully-automated terrain creation and robot locomotion testing apparatus, which we call the Systematic Creation of Arbitrary Terrain and Testing of Exploratory Robots (SCATTER, Fig. 2A). Using SCATTER, properties of heterogeneous multi-component substrates such as compaction, orientation, obstacle shape/size/distribution, and obstacle mobility within the substrate can be precisely controlled and varied to emulate a wide range of heterogeneous granular terrains. Since natural heterogeneous terrain comes in a huge variety of forms and it is impossible to test all random configurations, we used a model substrate with controlled heterogeneities – a granular test bed filled with small diameter spherical particles (the simplified "sand") and larger objects of various shapes (the simplified "boulders" and "rocks") embedded within (Fig. 2D). The relatively simple geometry and configuration of the model terrain makes it feasible to create repeatable states of granular media with controlled heterogeneity, and facilitates systematic exploration of heterogeneous ground properties.

The SCATTER system consists an air fluidized bed trackway, a universal jamming gripper[20] , and a high speed tracking system. The fluidized bed trackway was used to control the resistance of the fine grains. Using upward air flow through the trackway, the resistance of the sand can be varied over a large range, from greater than close packed compaction states to zero resistance.[21] The entire trackway was supported by an aluminum tiltable support frame and is actuated by two linear actuators (Firgelli, 454 kg, 61 cm stroke) such that the trackway could create inclined/declined granular environments.

To generate states of arbitrary heterogeneity, a 3-axis motor system was installed above the trackway, enabling the motor end-effector to move in three dimensions, driving a universal jamming gripper [20] (Fig. 2C) to programmed locations, creating arbitrary distributions of multi-size granular particles. The customized gripper assembly includes a balloon filled with granular material (a "universal jamming gripper"[20]), a support frame, and a HI-TEC servo motor (HSR-5980SG). The 3D-printed support frame connects the gripper to vacuum tubing through an air filter, enabling the granular material in the gripper balloon to switch between fluid-like and solid-like properties and grip objects of complex shapes. The support frame provides attachment from the gripper balloon to the servo disk, enabling the gripper assembly to adjust the robot orientation after each locomotion test. The system allowed distribution of boulders to designated locations before each locomotion test.

The legged robot we used in this study (Xplorer, Fig. 2B) has six 3D-printed C-shaped legs and uses a bio-inspired alternating tripod gait. The gait frequency of the robot was controlled by a DC motor (Micromo 1724-SR with IE2-1024 encoder) using pulse width modulation (PWM). A Hall effect sensor was attached to the robot body to control the initial leg phase and to track leg tip positions during the run. Robot kinematic information, including the x, y, z center of mass (CoM) position as well as the yaw, pitch, and roll angle, was obtained by tracking 3 IR-reflective markers attached to the robot using three top-view cameras (Naturalpoint, Flex13, 120 FPS). The cameras also monitored the location of the robot and the boulders before and after each test. This information was communicated to the motor system, so that the gripper could retrieve both the robot and boulders. The system recorded dorsal and lateral high speed reference videos that synchronized with the tracking data.

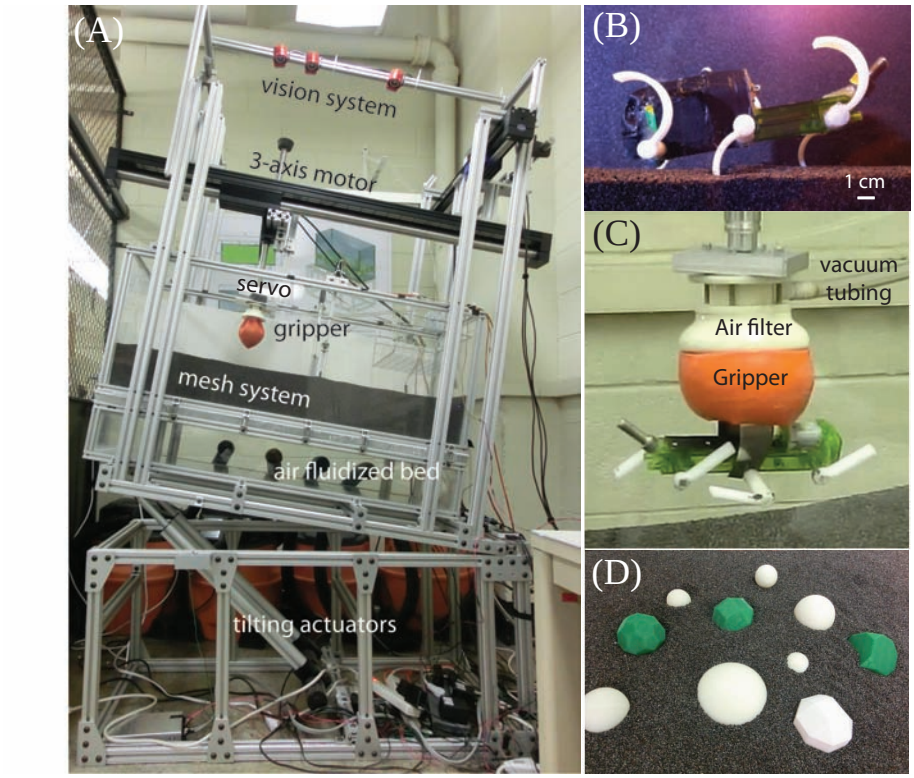

Figure 2. The SCATTER system. (A) The automated terrain creation and locomotion testing system, including the vision system, the 3-axis motor, the universal jamming gripper, the air fluidized bed and the tilting actuators. (B) The model locomotor, a C-legged hexapedal robot (Xplorer, 15 cm, 150 g) standing on homogeneous fine grains (1mm poppy seeds). (C) The universal jamming gripper lifting the robot. (D) An example of controlled heterogeneity for systematic variation in boulder shape and size – 1mm poppy seeds (the "sand") with larger 3D-printed spherical and polyhedral "boulders" embedded within.

All functions of the SCATTER system were controlled by a single integrated LabVIEW program. This terrain creation and robot locomotion testing system can currently take more than 200 locomotion tests in one day, without human intervention, allowing comprehensive and systematic exploration of the effects of arbitrary heterogeneity and spatial distribution, relative grain/grain and grain/locomotor sizes, robot limb size and kinematics on interaction modes and performance.

3. SCATTERING ANGLE DEPENDENCE ON LEG-BOULDER CONTACT POSITION

Using the SCATTER system, we systematically studied how a single boulder (a localized heterogeneity) affected the robot's trajectory.[1] For example, we compare robot trajectories during interaction with a single spherical boulder fixed at different burial depths in the sand (Fig. 3A). The boulder diameter was chosen to be 5 cm, comparable with the robot C-leg diameter (4 cm). We tested the robot trajectory for two different burial depths, one is a quarter-buried "High boulder" (Fig. 3B left, with three quarters of the boulder diameter, ≈ 3.75 cm, protruding from the granular surface) and the other is a three quarters buried "Low boulder" (Fig. 3B right, with only a quarter of the boulder diameter, ≈ 1.25 cm, protruding from the granular surface).

We fixed the robot's initial leg phase and systematically varied the initial fore-aft position of the robot such that the robot contacted with the boulder with different leg phases. We observed that the robot's trajectory was straight before interaction with the boulder, then exited at different angles (depending on initial conditions) after the interaction (Fig. 3C, E), as if the robot was "scattered" by the boulder. Interestingly, most of the robot trajectories were "attracted" to the boulder after the interaction. We noticed that the average trajectory deviation with "attraction" towards the boulder was significantly larger during high boulder interaction as compared to the low boulder interaction. When the robot contacted the high boulder, the interaction caused the robot to pitch and yaw significantly, in some cases the robot even flipped over backwards when the interaction occurred closer to the top region of the high boulder (lateral distance between robot centerline and boulder < 4 cm, with 0 cm being robot centerline passing through the boulder center). Therefore, in Fig. 3C $\sim$ F we only compare robot trajectories and scattering angle for initial lateral distances between 4 and 9 cm, with 9 cm being the point where the robot will no longer contact the boulder along its trajectory.

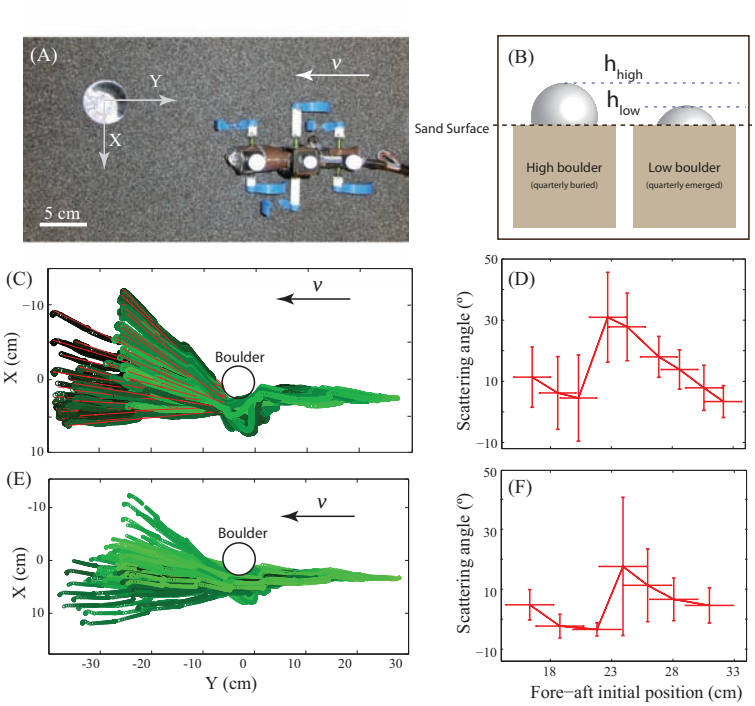

Figure 3. Robot interaction with single spherical boulder. (A) Experimental setup of the single boulder experiment. The center of the boulder is set as the origin. X and Y axis represents lateral and fore-aft direction. (B) Diagram of the two different boulder conditions tested here. The high boulder was slightly buried in the "sand" with three quarters of the boulder diameter (≈ 3.75 cm) protruded from the granular surface, whereas the low boulder was deeply buried with only a quarter of the boulder diameter, ≈ 1.25 cm, protruded from the granular surface. Both boulders were fixed at the burial depth and were not allowed to move during robot leg interaction. (C, E) Robot CoM trajectories for both high boulder setup (C) and low boulder setup (E). Trajectory color represents different initial fore-aft positions. Red lines are a linear fit of the robot's trajectories after boulder interaction, which were used to calculate the scattering angle. (D, F) Robot scattering angle after interaction with high boulder (D) and low boulder (F) as a function of the initial fore-aft distance between robot and the boulder. Postive scattering angle means that the robot turned to boulder (was "attracted") after the interaction and negative angle means the robot turned away from the boulder (was "repelled").

To quantitatively analyze the scattering effect of the boulder, we fit two lines to the trajectory, one before and one after the boulder interaction. These lines were used to characterize the trajectory's angular change (the scattering angle). We noticed that for both the high boulder and the low boulder the scattering angle depended sensitively on the robot's initial position. While the scattering magnitude upon the high boulder was significantly

larger as compared to the low boulder, the dependence of scattering angle upon robot initial fore-aft position was similar (Fig. 3D, F).

This sensitivity of scattering angle to robot initial position was likely due to different leg-boulder contact positions (or the boulder surface inclination at contact). The difference between the scattering magnitude between the low boulder and the high boulder was likely caused by the different boulder surface inclination angle at the same contact position on the boulder. In[1] we characterized the scattering angle as a function of the contact zones for a variety of boulders with variation in shape, orientation and roughness (Fig. 4), and we found that despite variation in boulder shape, roughness and orientation, the scattering angle sensitively depended on the leg-boulder contact zones, and this dependence exhibited similar characteristics for all boulders. We also noticed that most of the "attractive" zones were distributed on the front side of the boulder (Right front, Front, Left front), whereas most of the "repulsive" zones were distributed on the center or back side of the boulder (Left back, Top, Back, Right back). This is also consistent with our observation from the low boulder and high boulder experiment, and suggested that the fore-aft direction boulder surface inclination at contact was largely responsible for the sensitivity of scattering angle to robot initial positions (Fig. 3).

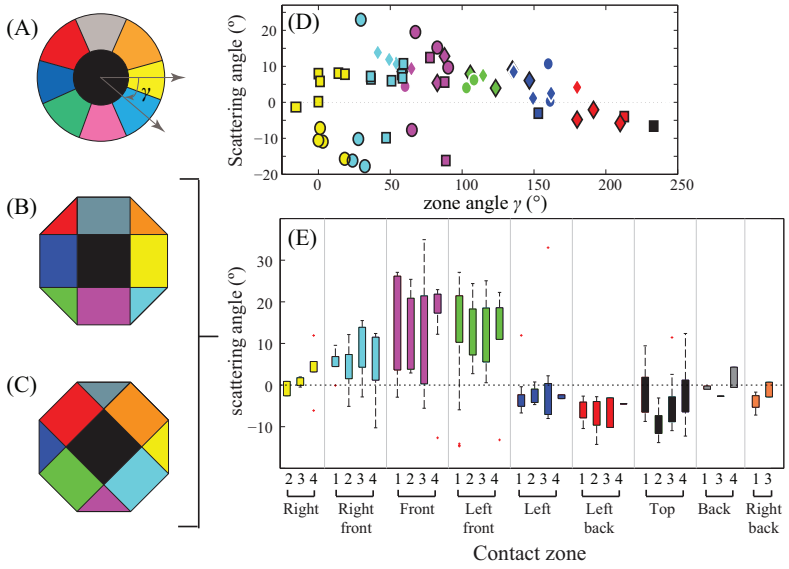

Figure 4. Scattering angle dependence on contact position for boulders of different shape, orientation and roughness. (A, B, C) Top view diagrams of the three boulder shapes and orientations, including a sphere (A), a 90 degree oriented rhombicuboctohedron (B), and a 45 degree oriented rhombicuboctohedron (C). For (B) and (C) we also tested two different roughness (plastic "smooth boulder" and sandpaper coated "rough boulder"). Different colors (yellow, cyan, purple, green, blue, red, black) corresponding to different contact zones (right, right-front, front, left-front, left, left-back, top), respectively. (D, E) Scattering angle vs. contact zone. (D) is spherical boulder and (E) are rhombicuboctohedral boulders with variation in orientation and roughness, including a rough 45 degree oriented rhombicuboctohedron (1), a smooth 45 degree oriented rhombicuboctohedron (2), a rough 90 degree oriented rhombicuboctohedron (3), and a smooth 90 degree oriented rhombicuboctohedron (4). Lower and upper limit of the central box in boxplot (E) represent the 25% and 75% quantile of the data, respectively. Color convention in (D, E) is the same as (A, B, C). Marker shape (square, diamond, circle) in (D) represents front, middle, rear leg contacted with the boulder, respectively. Markers without outlines indicate robot leg shaft contact. Figure adapted from [1] .

4. ANTICIPATORY BOULDER NEGOTIATION USING ROBOTIC TAIL

Based on the insensitivity in the scattering angle dependence upon contact zone among different boulder shape, roughness or orientation, we hypothesized that this general principle could be used as a prior knowledge to allow

low-cost platforms to perform anticipatory control. This is especially important for rapid running on complex terrains, where the sensing signals are usually noisy and sometimes not fast enough for the feedback controller to adjust robot posture from large perturbations, which could compromise the performance of feedback controllers. With anticipatory control, the robot can statistically estimate possible outcomes of the interaction before the disturbance, and therefore remain in a favorable configuration close to its natural, preferred movement pattern thereby allowing the feedback controller to better adjust robot locomotion. Here we demonstrate this scheme using a simple, tail-assisted substrate solidification approach, and we use a touch sensor embedded in the boulder to facilitate contact zone characterization.

4.1 Boulder sensing and tail actuation

To detect leg-boulder contact positions, we embedded a capacitive touch sensor (Freescale MPR121, 12 channels) into the 3D-printed rhombicuboctahedron boulder. Wire leads of 9 channels were attached to all polyhedral faces on the top half of the rhombicuboctahedron boulder, and fixed by adhesive copper tape (Figure 5A, B) that covered the different contact zones. The convex surfaces of all 6 robot legs were also covered by copper tape (Figure 5E) and grounded to trigger the capacitive touch sensor. Touch signals were acquired using Arduino Uno and then sent to LabVIEW via serial communication. When one or multiple zones were touched, the corresponding bit in the 2-byte signal was set to 1. This signal was then processed by LabVIEW and used to trigger different tail control behaviors.

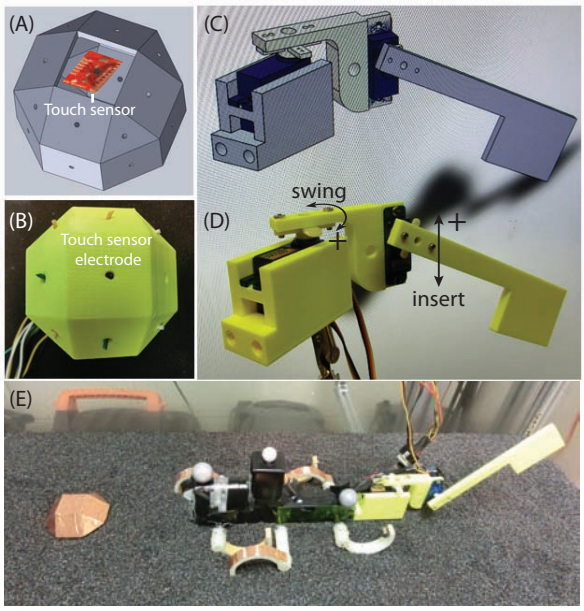

Figure 5. Boulder sensing and tail design in anticipatory control experiment. (A) Mechanical design diagram of a rhombicuboctahedron boulder with touch sensor embedded within. (B) 3D-printed "touch boulder" with electrodes from the embedded touch sensor wired to the boulder surface through 2 mm diameter holes. (C) Mechanical design of the robotic tail. (D) Integrated swing-insertion robotic tail controlled by two servo motors. (E) Experiment setup of the robot tail anticipatory control experiment. Touch sensor electrodes on each boulder zone were defined by copper tape. Robot legs were grounded to trigger touch sensor.

The robotic tail (Figure 5C, D) was actuated using two servo motors, one (HS-A5076HB) controlling the lateral swing of the tail, and another (HS-5055MG) controlling the vertical intrusion of the tail. Both servo motors were driven by a servo controller (Lynxmotion SSC-32) and controlled by pulse width modulation (PWM) in LabVIEW. The swing motor rotation was defined to be 0° when the tail was aligned with the robot body, and to be positive for clockwise (CW) rotation and negative for counterclockwise (CCW). The insertion motor rotation was defined to be 0° when the tail was horizontal, and to be positive for lifting upwards and negative for intruding downwards.

4.2 Trajectory control through tail induced substrate solidification

We implemented a simple control sequence (Figure 6A) to test the effectiveness of scattering correction using the tail. During the control sequence the tail moved in a rectangular trajectory in the sequential order of (1) Swing horizontally (CW/CCW) in air; (2) Insert vertically into sand; (3) Swing back horizontally within the sand; (4) Lift up. We characterized the resulting robot body turning angle β (Figure 6B, red squares) for a variety of tail motor swing and insertion angles, and surprisingly, we found that for all insertion angles that penetrated deeper than $-10°$, the body rotation angle mainly depended on tail motor swing angle and was insensitive to insertion angle.

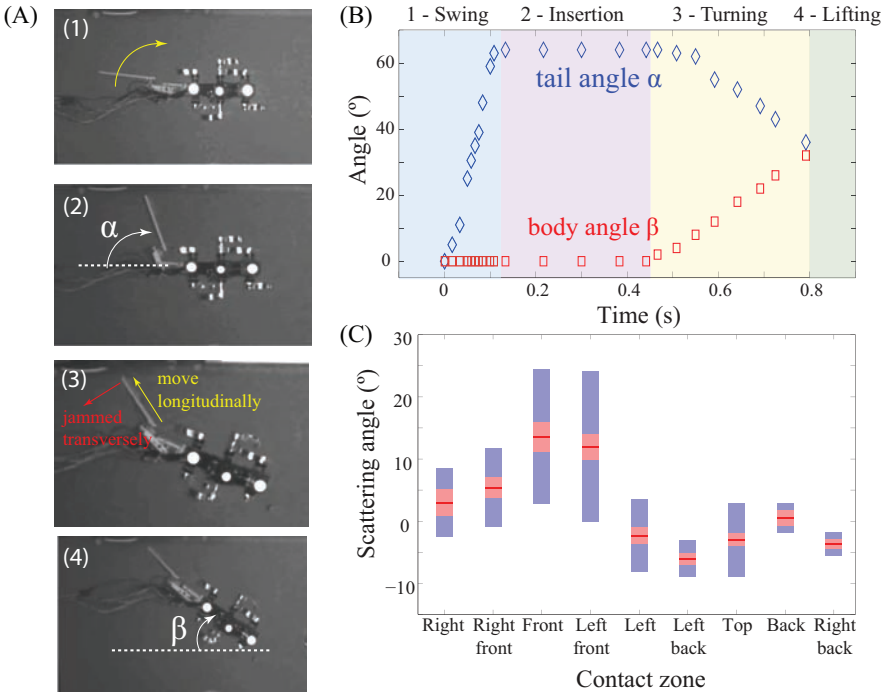

Figure 6. Tail control sequence and control signal that statistically estimated from scattering result. (A) Control sequence of the robotic tail. (1) Swing horizontally in air; (2) Insert vertically into sand; (3) Rotate back about swing motor axis, jamming the GM and constraint transversely to rotate the body; (4) After reorient the body, lift from the sand. (B) Tail angle (blue diamonds) and body angle (red squares) measured in world frame. (C) Statistical boxplot of the scattering angle vs. contact zone from experiment measurements shown in Figure 4E. Red line represents the mean of the scattering angle; pink box represents the 95% confidence interval; and blue box represents 1 s.d.. Non-overlapping confidence intervals indicate a significant difference at the chosen p-value of 5%. Tail control signal was set to be proportional to the mean scattering angle (red lines) but in opposite direction.

This independence of insertion angle is a result of the granular media reaching a jammed state. Granular jamming and solidification have been be used in robot and animal locomotion control to generate propulsion and achieve effective locomotion on granular substrates.[14,15,17] Unlike turning control in fluids where hydrodynamic response of the medium governs the turning dynamics, the solidification feature of granular material (i.e., the presence of a yield stress) provides a simple way to perform turning control, using the kinematically constrained relation between the robot body angle and tail swing angle. As shown in Figure 6A, during (3) the tail rotated about the swing tail motor axis, but due to the jammed granular media the tail could only extend longitudinally but not transversely. In this manner the resulting body rotation angle was kinematically constrained and could thus be controlled by only the initial tail swing angle. The tail swing angle, therefore, was set to be proportional,

but in the opposite direction, to the average scattering angle for each contact zone (Figure 6C), to correct for the body rotation during the scattering event. The intrusion angle was kept the same ($-30°$) for all contact zones, since the course correction angle was insensitive to tail insertion angle given that the tail intruded deeply enough to prevent significant fluidization of the granular media.

4.3 Scattering angle reduction with tail assisted anticipatory control

As a proof of concept, we did not attempt to correct for every incident of boulder contact, but instead looked to use minimal control effort to reduce the trajectory deviation on heterogeneous terrain. Our tests demonstrated that even with this simplified tail control, the scattering angle of the robot trajectory could be significantly reduced.

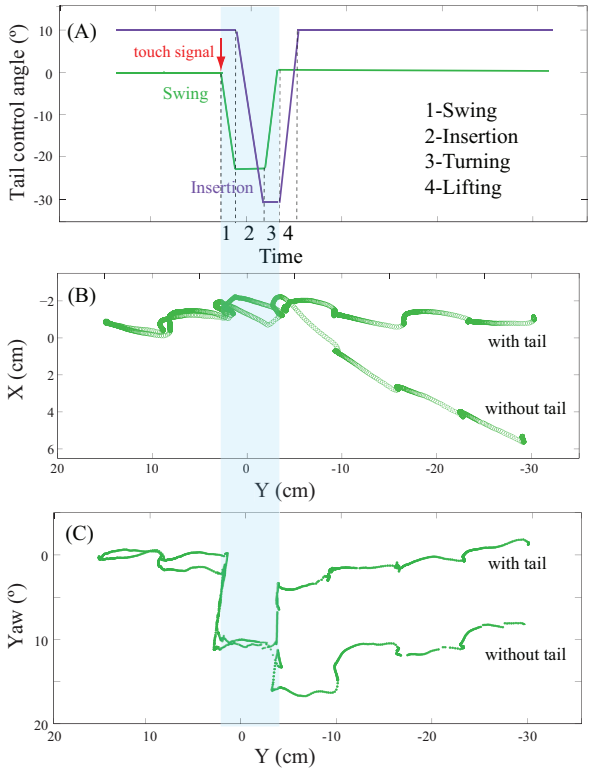

Figure 7. An example of two experimental runs with the same initial position and kinematics, one with tail anticipatory control and the other without. (A) Tail swing motor and insertion motor control signal. 1 - Tail rotated horizontally; 2 - Tail inserted $-30°$ into the sand; 3 - Tail rotated back to $0°$ in sand, jamming the GM to generate body rotation; (4) Tail lifted up to initial position. (B) Robot CoM trajectory comparison between open loop control and tail anticipatory control. (C) Robot body yaw angle comparison between open loop control and tail anticipatory control.

Figure 7 shows an example of two experimental runs with the same initial and kinematics settings, one with tail anticipatory control and the other without. Before the robot started moving, the tail swing motor was set to $0°$ and the insertion motor angle was set to $10°$ (slightly lifted above the sand surface). For the tests with tail control enabled, upon the first leg-boulder contact (triggered by the touch sensor signal), as shown in Figure 7A, the tail rotated horizontally (1-Swing) to the prescribed angle based on the scattering angle predicted by the zone of contact, subsequentially descended into the GM (2-Insertion), then rotated back to $0°$ about the swing motor axis, while remaining transversely constrained in the jammed GM and generating a body rotation to reorient the robot (3-Turning). Following the body rotation, the tail was lifted from the GM (4-Lifting).

We see from Figure 7 that before the leg-boulder contact, the two robot trajectories were similar. However, as the robot leg contacted the boulder, the robot without tail control slipped off the boulder, generating a lateral impulse that caused $> 10^\circ$ change in the yaw angle of the robot (Figure 7B without tail), and leading to a CoM trajectory that deviated from the initial direction (Figure 7C without tail). The tailed robot began the anticipatory control (Figure 7A) upon leg-boulder contact, and successfully reduced the scattering angle within the same step (Figure 7C with tail) resulting in a straight trajectory (Figure 7B with tail), similar to the robot trajectory on homogeneous granular ground.

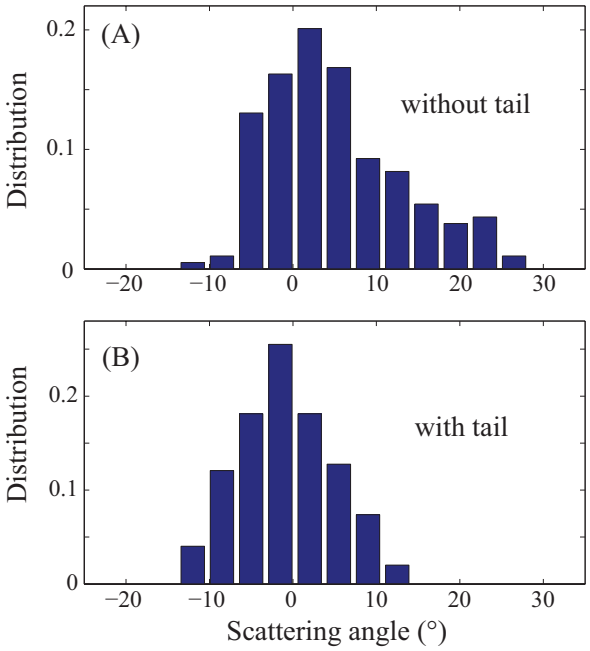

Figure 8. A comparison of scattering angle distribution between with (A) and without (B) tail anticipatory control. The robot trajectory deviation with tail control was reduced from a maximum value of $\approx 28^\circ$ to $\approx 13^\circ$, eliminating large attractive scattering angle components.

Figure 8 shows the difference in scattering angle distribution between with and without tail anticipatory control over 300 runs. With anticipatory control, the scattering angle was significantly reduced from maximum values reaching $\approx 28^\circ$ to $\approx 13^\circ$, eliminating large attractive scattering angles and reducing the average trajectory deviation to close to zero. The $\pm 10^\circ$ distribution of uncorrected scattering angles was a consequence of the simplified control scheme. That is, the tail performed anticipatory control only upon the first contact on the boulder, but there could be multiple leg-boulder interactions during one run, with leg sliding from one contact zone to another, or multiple legs contacting on different boulder zones at the same time. In future work, we will investigate the multi-interactions effect, and model the robot-boulder interaction mode based on the local boulder surface angle, to allow for more accurate and dynamic control of locomotion. Also, we noticed that the scattering correction was relatively less effective for small scattering angles (e.g., $< 5^\circ$). This is largely due to the delayed material response during the tail induced solidification. In future work, we will systematically characterize the tail's morphological and kinematic parameters, to increase the effectiveness in producing GM jamming.

5. CONCLUSION

We developed an anticipatory control scheme which relied on granular solidification and scattering knowledge. We obtained the scattering information by using a previously developed SCATTER system, which can precisely control and automatically vary properties of the heterogeneous granular substrates. Analysis of robot trajectories in single boulder experiments revealed that the interaction with a single, localized boulder could be modeled

as a scattering effect with attractive and repulsive features. The scattering angle depended sensitively on the leg-boulder contact position, but remarkably, this dependence was relatively insensitive to boulder shape, orientation and roughness. We demonstrated that by utilizing this scattering insensitivity, the robot could perform a tail-assisted anticipatory control using a tail induced substrate solidification, and significantly reduce the trajectory deviation caused by boulder interaction. Our scattering study provides a better understanding of the complex interaction between the robot and the heterogeneous ground, and allows robots to evaluate obstacle traversability and predict the probability of outcomes (e.g., possible failure, trajectory deviation, etc.) of different locomotion modes before perturbations. In this manner even simple, low-cost robots can perform successful anticipatory control and manipulate their environments to remain in a favorable locomotor configuration and avoid catastrophic failures.

6. ACKNOWLEDGMENTS

This work is supported by the Army Research Laboratory (ARL) Micro Autonomous Systems and Technology (MAST) Collaborative Technology Alliance (CTA) and the Defense Advanced Research Projects Agency (DARPA) Young Faculty Award (YFA). We thank Andrei Savu and Kevin Daffon for help with test bed construction, Duncan Hathaway for help with preliminary data collection. We thank Daniel E. Koditschek, Paul Umbanhowar, Nick Gravish and Jeff Aguilar for helpful discussion.

REFERENCES

1. F. Qian and D. I. Goldman, "The dynamics of legged locomotion in heterogeneous terrain: universal scattering and sensitivity to initial conditions," *Robotics: Science and Systems (RSS)* . in review.
2. "https://www.youtube.com/watch?v=s1wmplbvgjg."
3. A. E. Patla, S. D. Prentice, S. Rietdyk, F. Allard, and C. Martin, "What guides the selection of alternate foot placement during locomotion in humans," *Experimental Brain Research* **128**, pp. 441–450, Oct. 1999.
4. A. A. Biewener and M. A. Daley, "Unsteady locomotion: integrating muscle function with whole body dynamics and neuromuscular control.," *The Journal of Experimental Biology* **210**, pp. 2949–2960, Sept. 2007.
5. H. Cruse, C. Bartling, G. Cymbalyuk, J. Dean, and M. Dreifert, "A modular artificial neural net for controlling a six-legged walking system," *Biological cybernetics* **72**(5), pp. 421–430, 1995.
6. A. Tryba and R. Ritzmann, "Multi-joint coordination during walking and foothold searching in the Blaberus cockroach. I. Kinematics and electromyograms," *Journal of neurophysiology* **83**(6), pp. 3323–3336, 2000.
7. S. Sponberg and R. J. Full, "Neuromechanical response of musculo-skeletal structures in cockroaches during rapid running on rough terrain.," *The Journal of Experimental Biology* **211**, pp. 433–446, Feb. 2008.
8. G. Meirion-Griffith and M. Spenko, "Comprehensive pressure-sinkage model for small-wheeled unmanned ground vehicles on dilative, deformable terrain," *2012 IEEE International Conference on Robotics and Automation* , pp. 4052–4057, May 2012.
9. G. Heiken, D. Vaniman, and B. M. French, *Lunar sourcebook: A user's guide to the Moon*, CUP Archive, 1991.
10. J. Kuffner, S. Kagami, K. Nishiwaki, M. Inaba, and H. Inoue, "Online footstep planning for humanoid robots," *Proceedings of IEEE International Conference on Robotics and Automation (ICRA)* **1**, pp. 932–937, 2003.
11. T. Bhattacharjee and P. Grice, "A Robotic System for Reaching in Dense Clutter that Integrates Model Predictive Control, Learning, Haptic Mapping, and Planning," *Proceedings of the 3rd IEEE/RSJ International Conference on Intelligent Robots and Systems (IROS)* , 2014.
12. M. G. Bekker, "Theory of land locomotion," *University of Michigan* , 1956.
13. J. Y. Wong, *Terramechanics and off-road vehicles*, Elsevier, 1989.
14. C. Li, P. B. Umbanhowar, H. Komsuoglu, D. E. Koditschek, and D. I. Goldman, "Sensitive dependence of the motion of a legged robot on granular media.," *Proceedings of the National Academy of Sciences* **106**, pp. 3029–3034, Mar. 2009.

15. N. Mazouchova, P. B. Umbanhowar, and D. I. Goldman, "Flipper-driven terrestrial locomotion of a sea turtle-inspired robot.," *Bioinspiration & biomimetics* **8**, p. 026007, June 2013.
16. R. D. Maladen, Y. Ding, C. Li, and D. I. Goldman, "Undulatory swimming in sand: subsurface locomotion of the sandfish lizard," *science* **325**(5938), pp. 314–318, 2009.
17. H. Marvi, C. Gong, N. Gravish, H. Astley, M. Travers, R. L. Hatton, J. R. Mendelson, H. Choset, D. L. Hu, and D. I. Goldman, "Sidewinding with minimal slip: snake and robot ascent of sandy slopes.," *Science (New York, N.Y.)* **346**, pp. 224–9, Oct. 2014.
18. C. Li, T. Zhang, and D. I. Goldman, "A terradynamics of legged locomotion on granular media.," *Science* **339**, pp. 1408–1412, Mar. 2013.
19. F. Qian, K. Daffon, T. Zhang, and D. I. Goldman, "An automated system for systematic testing of locomotion on heterogeneous granular media," *in Proceedings of the 16th International Conference on Climbing and Walking Robots (CLAWAR)* , pp. 1–8, 2013.
20. E. Brown, N. Rodenberg, J. Amend, A. Mozeika, E. Steltz, M. R. Zakin, H. Lipson, and H. M. Jaeger, "Universal robotic gripper based on the jamming of granular material," *Proceedings of the National Academy of Sciences* **107**, pp. 18809–18814, Oct. 2010.
21. F. Qian, T. Zhang, W. Korff, P. B. Umbanhowar, R. J. Full, and D. I. Goldman, "Principles of Appendage Design in Robots and Animals Determining Terradynamic Performance on flowable ground," *Bioinspiration & biomimetics* . in review.